Probing the Dynamic Nature of Self-Assembling Cyclic Peptide-Polymer Nanotubes in Solution and in Mammalian Cells

*Julia Y Rho, Johannes C Brendel, Liam R MacFarlane, Edward D H Mansfield, Raoul Peltier, Sarah Rogers, Matthias Hartlieb, Sébastien Perrier**

J. Y. Rho, Dr. J. C. Brendel, Dr. E. D. H. Mansfield, Dr. R. Peltier, Dr. M. Hartlieb, Prof. S. Perrier: Department of Chemistry, University of Warwick, Gibbet Hill Road, Coventry CV4 7AL, United Kingdom.

Prof. S. Perrier: Faculty of Pharmacy and Pharmaceutical Sciences, Monash University, 381 Royal Parade, Parkville, VIC 3052, Australia.

L. R. MacFarlane: School of Chemistry, University of Bristol, Bristol, Cantock's Close, BS8 ITS, United Kingdom.

Dr. S. Rogers: ISIS Neutron Facility, Rutherford Appleton Laboratory, Harwell Oxford, Didcot OX11 0QX, United Kingdom.

Prof. S. Perrier: Warwick Medical School, The University of Warwick, Coventry CV4 7AL, U.K.;

*Corresponding author: s.perrier@warwick.ac.uk

Keywords: cyclic peptide nanotubes, Förster resonance energy transfer, supramolecular polymers, peptide polymer conjugates, self-assembly;

Abstract

Self-assembling cyclic peptide polymer nanotubes have emerged as a fascinating supramolecular system, well suited for a diverse range of biomedical applications. Due to their well-defined diameter, tunable peptide anatomy, and ability to disassemble *in situ,* they have been investigated as promising materials for numerous applications including biosensors, antimicrobials, and drug delivery. Despite this continuous effort, the underlying mechanisms of assembly and disassembly are still not fully understood. In particular, the exchange of units between individual assembled nanotubes has been overlooked so far, despite its knowledge being essential for understanding their behaviour in different environments. To investigate the dynamic nature of these systems, we synthesized cyclic peptide polymer nanotubes conjugated with complementary dyes, which undergo a Förster resonance energy transfer (FRET) in close proximity. Using model conjugates we were not only able to demonstrate that their self-assembly is highly dynamic and not kinetically trapped, but also that the self-assembly of the conjugates is strongly influenced by both solvent and concentration. Additionally, the versatility of the FRET system allowed us to study the dynamic exchange of these systems in mammalian cells *in vitro* using confocal microscopy, demonstrating the exchange of subunits between assembled nanotubes in the highly complex environment of a cell.

Introduction

Since the discovery of natural supramolecular polymers,[1] whereby the manipulation of chemistry on a molecular level can influence the formation of larger more versatile structures, there has been a drive to replicate such systems synthetically. For this reason, many synthetic self-assembling systems, which utilise non-covalent interactions, have culminated in the formation of an extraordinary library of nanoscale architectures such as nanofibers,[2] nanotubes,[3] nanorods,[4] and twisted nanoribbons.[5] Understanding these systems and predicting their behaviour is essential to maximising their potential for a diverse range of applications such as electronics,[6] bio-sensing[7] or drug delivery.[8] The fundamental nature of supramolecular polymer assemblies has been extensively studied by Meijer, Stupp and Aida.[9] Early work in this field differentiated between, isodesmic or cooperative self-

assembly mechanisms.[10] The driving forces behind the formation and propagation of these assemblies typically includes hydrogen bonding, metal coordination, π-π stacking, inclusion complexes and Van der Waals, electrostatic and hydrophobic interactions.[11] For biological applications, a focus has been placed on replicating the hydrogen bonding interactions widely found in living systems, most notably in the structure of proteins.[12] Stupp *et al.* have studied the selective assembly and disassembly of self-assembling peptide amphiphiles, in different environments, that rely on both hydrogen bonding and hydrophobic interactions as driving forces of the assembly process.[2b] Exploiting the dynamic properties to depolymerise supramolecular systems, a feature many living systems use to provide vital biological functions,[13] is next challenge in mimicking the level of complexity exhibited in nature.

Recently, attention has focused on designing supramolecular systems that are increasingly relevant for biomedical applications.[14] A highly versatile system in this context are self-assembling cyclic peptide (CP) nanotubes. The alternating D- and L- amino acid confirmation of the peptide leads to the formation of a flat disc-like structure. Perpendicular to the plane of the cyclic peptide ring the amide bonds participate in hydrogen bonding to form a nanotubular assembly.[3] These systems have gained much attention due to their potential biological applications as antimicrobial materials,[15] biosensors[16] and drug delivery vehicles.[17] Conjugation of water-soluble polymers to these peptides significantly improves their solubility, further widening the range of biological applications.[14b] As for most supramolecular structures, it remains unclear whether these self-assembled nanotubes are kinetically stable or are constantly exchanging subunits to reach a kinetic equilibrium. As this behaviour is of paramount importance to predict their performance in future *in vitro* and *in vivo* studies, an in-depth study of the dynamic nature of CP-polymer conjugates is critical.

Herein, we designed CP-polymer conjugates modified with fluorescent dyes and used Förster resonance energy transfer (FRET) to probe the dynamic nature of the resulting nanotubes. Fluorescence is a powerful tool to study close intramolecular interactions and investigate the dynamic behaviour of supramolecular systems. [18] [19] In the context of cyclic peptides, Granja *et al.* previously

employed FRET to study the hydrogen-bonding interaction of small dimeric cyclic peptides.[20] In here, we propose to use FRET to gain an insight into the stacking of cyclic peptide nanotubes (CPNTs) *in situ* and provide vital information about the dynamics of these one-dimensional supramolecular structures. To gain a detailed understanding, key parameters such as solvent and concentration were varied, and their influence on the assembly process studied. In addition, the use of FRET allowed us to observe the behaviour of these nanotubes in mammalian cells *in vitro*, thus providing essential information about their dynamics in a complex biological environment.

Results and Discussion

Synthesis of cyclic peptide-polymer dye conjugate

In order to investigate the dynamics of self-assembled cyclic peptide polymer nanotubes, a new class of dye conjugated peptides were synthesised. To infer information about the kinetic exchange of these systems, each cyclic peptide required the conjugation of a single FRET dye to its periphery. Using a 'bottom up' approach, a sequence of amino acids was designed to yield an asymmetric cyclic peptide, which could be used to conjugate both a dye and polymer in an orthogonal manner. The bespoke asymmetric cyclic peptide (**3**, Scheme 1) used in this study, contained both an azide and amide moiety on its periphery (see Supplementary information, Figure S1 for details).

Synthesis of the peptide was carried out *via* solid-phase peptide synthesis using Fmoc-deprotection chemistry. Cyclisation of the linear peptide into peptide 2 (Scheme 1, Figure S1) was then performed under dilute conditions to avoid intermolecular reactions. Full characterisation of these compounds can be found in the supplementary information (Figure S1-4). The attachment of the FRET dyes to the cyclic peptide was achieved *via N*-hydroxysuccinimide (NHS)-amine coupling. The efficiency of this step was assessed using High Pressure Liquid Chromatography (HPLC) and was shown to be quantitative, enabling the FRET emission to directly inform us of the exchange kinetics of the supramolecular system. Cyanine FRET dyes Cy3 and Cy5 were chosen as the FRET pair as their high extinction coefficients enables the detection of FRET at very low concentrations.[21] Additionally, the

spectral overlap of these dyes is ideal to avoid undesirable excitation of the acceptor. Characterisation of the dye-functionalised CP-polymer conjugates was done *via* HPLC equipped with ultraviolet (UV) and fluorescence detection (Supplementary information, Figure S7-8), as well as Electrospray Ionisation - Time of Flight (ESI-ToF) mass spectrometry (Supplementary information, Figure S4-5). A non-fluorescent conjugate was also synthesised as a control. For this conjugate to best mimic the self-assembly of the dye-functionalized conjugates, the free amine of the Lysine residue was converted to an amide group, by conjugation with valeric acid using the peptide coupling agent HATU (Scheme 1). The alkyl chain on the valeric acid replicates the alkyl linker on the NHS functionalised dyes.

Conjugation of a water soluble polymer to the cyclic peptide helps to control the length of the tubular assembly and prevents lateral aggregation, in addition to improving the solubility of these otherwise insoluble nanotubes.[22] For this model system, a linear poly(ethylene glycol) (PEG 20 kg mol^{-1}) end-functionalized with an amine group was chosen. Using copper-free strain promoted alkyne-azide coupling,[23] the cyclic peptide conjugates were functionalised with a free NHS group, which was subsequently used to attach the amine-bearing PEG. HPLC and ESI-ToF analyses confirm the successful attachment of the linker and polymer after each step (Supplementary information, Figures S4-9). A simplified representation of the conjugation reactions is shown in Scheme 1 and detailed reaction scheme can be found in Figure S1. While the cyclic peptide alone is only soluble in DMSO, DMF and TFA, the CP-polymer conjugates proved to be soluble in a range of solvents such as water and toluene.

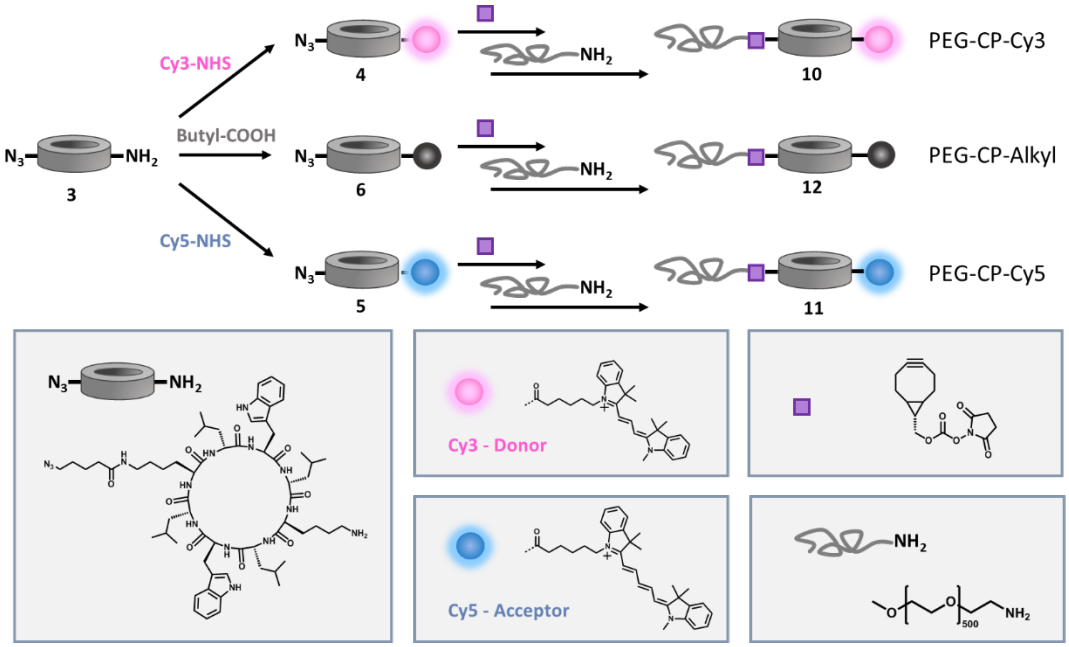

Scheme 1. Schematic representation of the synthesis of cyclic peptide-dye-polymer conjugates.

Characterisation of the self-assembling cyclic peptide conjugates

Hydrogen bonding between the amide bonds is known to drive the self-assembly of the CPNTs. However, the length of the formed nanotube can be influenced by number of different factors such as composition and position of the amino acids, as well as polymer grafting.[14b] Herein, the morphology of the resulting CP-polymer conjugates were analysed using small angle neutron scattering (SANS), Static Light Scattering (SLS) and Transmission Electron Microscopy (TEM).

SANS is a powerful technique to characterise complex systems in order to understand any structural parameters, interactions, and changes due to environmental stimuli occurring in solution.[24] Previously, our group has used SANS to analyse a wide-range of CPNTs in different solvents, polymer conjugations, and in response to different stimuli (pH and temperature).[25] Here, SANS was used to confirm the formation of nanotubes for a mixture of conjugates **10** and **12**, and to analyse how the presence of a fluorophore affected their stacking potential compared to the non-dye conjugated control (PEG-CP-Alkyl, **11**).

Figure 1A shows the reduced, corrected scattering data for the control and the dye conjugated peptide system. From the fit, the length of each nanotube could be obtained. The data were initially fitted with either a cylinder or a core-shell cylinder model form factors, however, a statistically reliable fit was not obtained. As a result, a hairy-cylinder model was used that combines the form factors for a micelle with a rod-like core and attached flexible polymer chains, with a high degree of accuracy in both cases (Supplementary information, Figure S15). The core-radius has been shown to be 0.34 nm in previous studies and was used as a fixed parameter in the fitting process.[25a] From the values obtained, the number of aggregation (N_{agg}) can be determined by dividing the length of the tube by the distance between two single cyclic peptide unimers (0.47 nm), shown in Table 1.[25a, 26] Visually analysing the scattering profiles reveals a major difference in the Guinier region (q = 0.00416 - 0.01). Given that the Guinier region provides information on larger structures within the system, deviations here indicate nanotubes of different lengths. The control has a higher intensity at q^{-1}, suggesting the formation of longer nanotubes, which is demonstrated in the fits. The scattering due to the dye-conjugated peptide on the other hand exhibits a change in slope, thus suggesting tubes of a finite length exist. The length of the tubes was found to be 117 nm, compared to 89 nm for the control and mixed system, respectively.

In addition to SANS, SLS experiments were used to determine the N_{agg} for the non-dye conjugated system in a range of concentrations (Figure S15). The dye conjugates could not be measured directly as the wavelength of the laser used for SLS (633nm) overlaps with the dye excitations (570nm and 646nm for Cy3 and Cy5, respectively). The N_{agg} of non-dye conjugated system was then used as a floating variable in the fitting process.

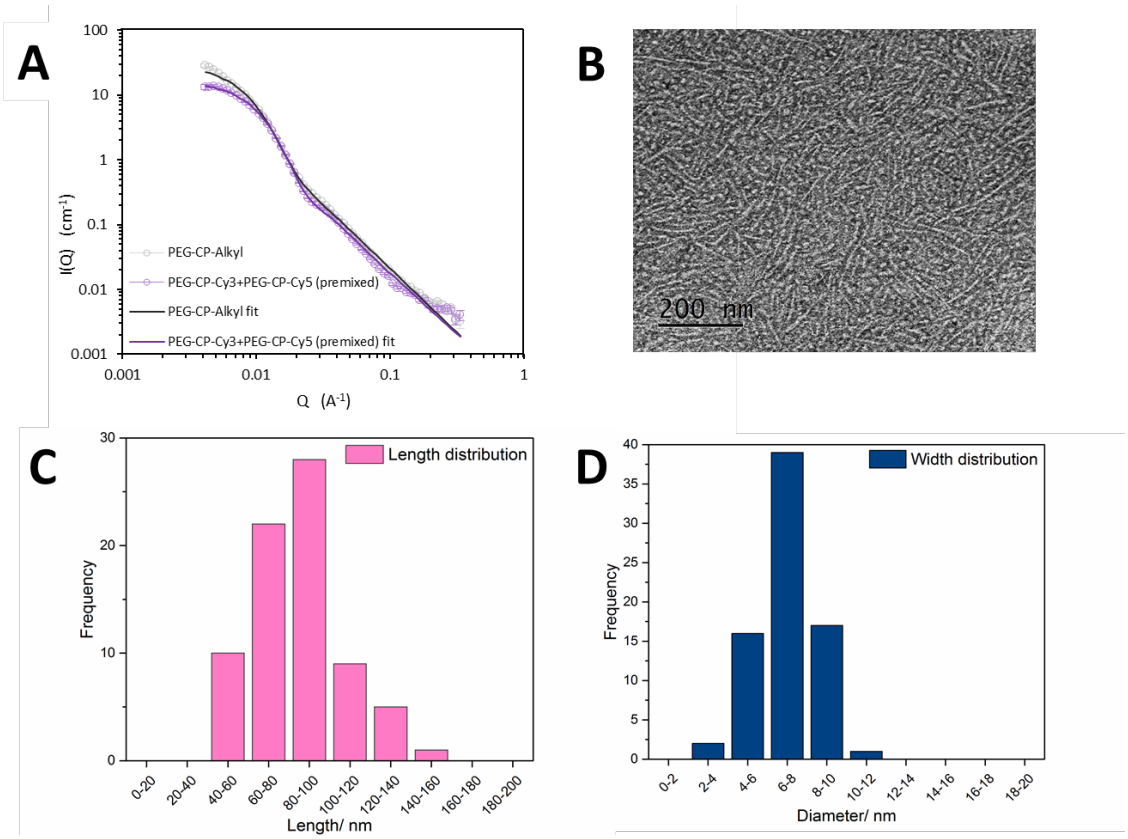

Figure 1. A) Reduced SANS scattering data for the PEG-CP-Alkyl (Control) and (Premixed) PEG-CP-Cy3 and PEG-CP-Cy5 system. The lines correspond to a fit to the hairy cylinder model. B) TEM image of cyclic peptide-polymer-dye conjugate (PEG-CP-Cy3) stained with UOAc. Distribution of nanotubular C) lengths and D) diameters extracted from TEM.

Table 1. Summary on the characterisation of CPNTs using SANS and TEM. TEM values are represented as mean lengths and diameters ± standard deviation of 37 individual nanotubes.

Sample	**Length (SANS)/ nm**	**N_{agg} (SANS)/ nm**	**Length (TEM)/ nm**	**N_{agg} (TEM)/ nm**	**Diameter (TEM)/ nm**
PEG-CP-Cy3	-	-	85.0 (± 22.3)	180.9	7.1 (± 1.5)
PEG-CP-Cy5	-	-	81.8 (± 14.1)	174.0	8.4 (± 2.2)

PEG-CP-Cy3 and PEG-CP-Cy5 (Premixed)	89.0	189.3	-	-	-
PEG-CP-Alkyl	116.9	248.8	117.7 (± 32.0)	250.4	15.5 (± 3.7)

The data presented here clearly confirm that both the control (PEG-CP-Alkyl) and mixed systems (PEG-CP-Cy3 and PEG-CP-Cy5) form long nanotubular aggregates of similar size *in situ*. Discrepancy in the sizes can be attributed the presence of bulky and charged dye (Cy3 or Cy5). Yet, the variation remains minor, possibly due to the distance between the dye and the cyclic peptide created by the linker.

Using TEM the nanotubular morphology observed in SANS was independently confirmed. Samples were prepared from pure water (1 mg/mL) using the drop casting method. The low electron density of the peptide-dye-polymer conjugates made obtaining TEM images of these compounds very challenging, thus negative staining of samples dropcast on thin (4 nm) carbon-coated copper grids was used. Images are presented in Fig 1B. The formation of one-dimensional structures can be evidently seen for all three presented cyclic peptides (Figure 1B and S14). Upon statistical analysis of the TEM images using ImageJ, a very narrow distribution with a mean diameter of 7.1 nm was determined for PEG-CP-Cy3 (Figure 1D). This finding is consistent with the formation of single conjugated nanotubes. The diameter of the PEG-CP-Cy5 was relatively similar (mean diameter = 8.4 nm), however a larger value was obtained for PEG-CP-Alkyl (mean diameter = 15.5 nm). This could be associated to lateral aggregation upon removal of the solvent. The distribution of nanotube lengths was found to be wider (mean length = 85.0 nm for Cy3-peptide, and 81.8 nm for Cy5-peptide), which is to be expected in a self-assembled system (Figure 1C). Distribution for PEG-CP-Cy5 and PEG-CP-Alkyl and can be found in Figure S14.

Spectrochemical properties of dye conjugated cyclic peptides

Following synthesis and characterisation, FRET was used to probe the dynamic nature of these supramolecular systems. The FRET emission of the acceptor dye (PEG-CP-Cy5) only occurs when specific requirements are met. Firstly, the emission spectra of the donor (PEG-CP-Cy3) should overlap with the absorption spectra of the acceptor enabling the fluorescence of the donor to excite the acceptor. The Cyanine dye FRET pair Cy3 and Cy5 typically fulfil these requisites and have been extensively used due to their high excitation coefficients, biocompatibility and ideal spectral overlap.[27] The absorption and emission spectra of PEG-CP-Cy3 and PEG-CP-Cy5 show that the conjugates conserve these properties (Figures S10-11). To reduce direct excitation of the acceptor dye in the subsequent FRET studies, which could also lead to acceptor emission, the donor was excited at 500 nm instead of its absorption maxima. Secondly, FRET will only take place if the donor and acceptor (Cy3 and Cy5 respectively) are close enough in space for the energy transfer to take place, typically 10-100Å.[21, 28] The average distance between two CPs has previously been reported to be 4.7Å and the pore diameter of the CP around 7.5 Å.[14b, 29] Therefore, an energy transfer for the presented system is expected if both dyes are incorporated into the same nanotube upon mixing. When these conditions are fulfilled, the energy transfer translates into a decrease in donor emission and an increase in the acceptor emission.

Here, FRET studies were carried out by comparing a mixture of PEG-CP-Cy3 and PEG-CP-Cy5, and a mixture of the free dyes in solution (Cy3 and Cy5) as a control. Mixing the dyes alone resulted in no change in the emission spectra over 30 minutes, which can be attributed to the dyes being too far from one another in solution (Figure S18). In comparison, the emission of PEG-CP-Cy5 increased and the emission of PEG-CP-Cy5 decreased over time upon mixing (Figure 2B). This behaviour is indicative of the formation of FRET pairs, resulting from the exchange of monomer units or small segments of peptide between the formed nanotubes. The increase over time indicates that CPs dynamically exchange between different nanotubes to form increasingly mixed nanotubes, as no self-assembly and exchange would result in no FRET occurring. A schematic depiction of mixed cyclic peptide-polymer-dye conjugates can be found in Figure 2A.

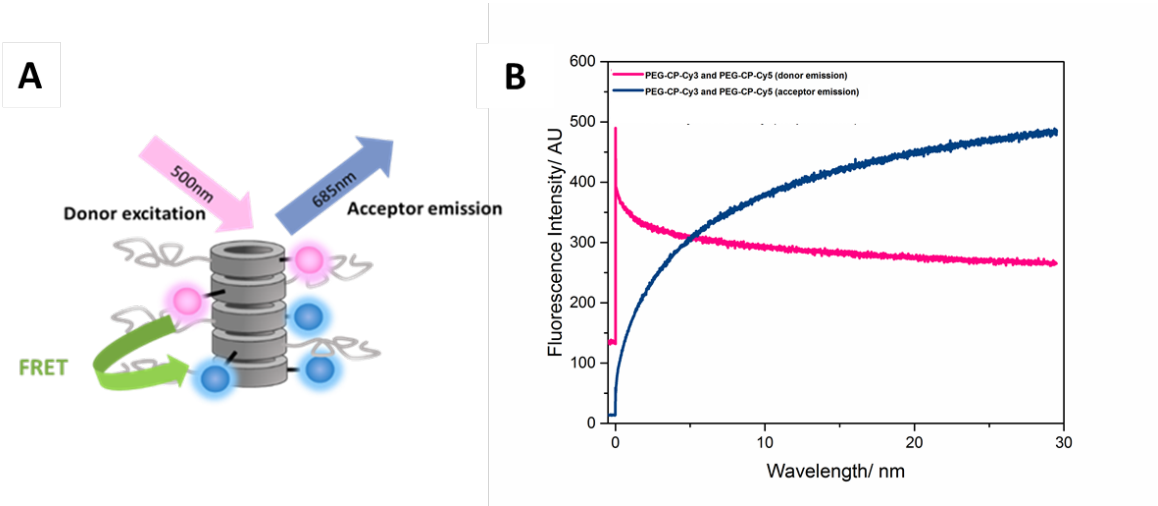

Figure 2. A) Schematic depiction of the FRET occurring in cyclic peptide nanotubes containing donor (Cy3) as well as acceptor (Cy5) dye molecules. B) Fluorescence donor and acceptor emission upon mixing the free dyes (Cy3 and Cy5) and the self-assembling dye conjugates (PEG-CP-Cy3 and PEG-CP-Cy5) in water.

Solvent dependent dynamic unimer exchange of CPNT

Using the FRET system outlined above we can further probe the dynamics of the dye conjugates (PEG-CP-Cy3 and PEG-CP-Cy5) in a range of different solvent environments. Our group has previously shown that cyclic peptides form shorter nanotubes in more hydrogen bond competitive solvents.[30] This is due to the solvent molecules competitively binding to the hydrogen bonding sites on the cyclic peptide required for stacking.

In order to investigate these dynamics, stock solutions of PEG-CP-Cy3 (**10**) and PEG-CP-Cy5 (**11**) were made in DMF, water and toluene which have a range of different properties. Emission spectra, upon mixing the dye conjugates (PEG-CP-Cy3 and PEG-CP-Cy5) in a 1:1 volume ratio were taken at several different time intervals (Figure 3B) until a plateau was reached. Emission was then expressed as a FRET ratio, calculated using equation 1.[31]

$$E_{rel.} = \frac{I_A}{I_D + I_A} \quad (1)$$

Where I_A and I_D are the total acceptor and donor fluorescence intensities respectively (Fig 3).

Again, the change in emission associated with FRET (i.e. decrease in the donor and increase in the acceptor emission) was observed, with the exception of DMF, whereas in water and toluene a clear increase can be observed, showing FRET is occurring. Interestingly, the rate at which FRET occurs appears to be different for both water and toluene (Fig 3C). In both solvents where conjugates are expected to assemble, the FRET ratio increases as a function of time, and therefore show the cyclic peptides dynamically exchanging to form progressively mixed nanotubes. This increase in FRET ratio eventually reaches a plateau whereby no further net mixing was observed and an equilibrium is maintained. The final FRET ratio of the equilibrium in different solvents clearly varies, and is postulated to be a result of the solvatochromic effects of the solvent, and/or the different lengths the nanotube assemblies. In addition, an insufficient exchange of CPs can lead to a lower final FRET ratio. The solvent dependent exchange kinetics were determined by modelling the increase in FRET ratio to a bi-exponential decay function, using OriginPro, providing two rate constants. A single exponential function yielded poor fits (R^2 <0.9). Other FRET ratio kinetics in literature have also reported to require bi-functional models.[31a] This suggests that there are two different mixing processes occurring, an initial fast rate of mixing (K_1) followed by a slower gradual exchange between assemblies (K_2) until an equilibrium is reached. No rate constants could be determined for DMF as no increase over time was observed as the FRET ratio of < 0.l was reached instantaneously after mixing.

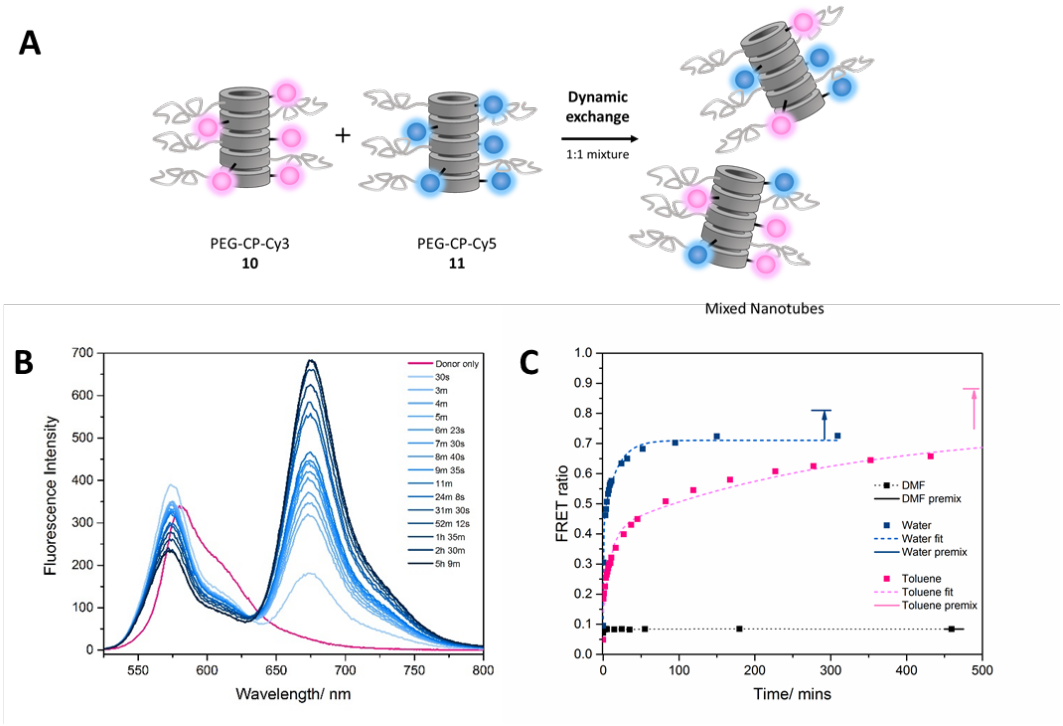

Figure 3. A) Schematic depiction of the FRET studies. Preassembled individual cyclic peptide-dye-polymer conjugates in water (left) and a 1:1 mixture of both conjugates after the assemblies are left to dynamically exchange (right). B) Fluorescence emission spectra of PEG-CP-Cy3 and PEG-CP-Cy5 upon mixing in water and C) Normalised FRET ratio of the mixed system in DMF, water and toluene. Toluene plateau was reached after 6 days (see Supplementary information, Figure S13).

In a highly hydrogen competitive solvent such as dimethylformamide (DMF), mainly unimeric species or small aggregates were expected,[30] which is corroborated by the lack of change in FRET ratio upon mixing (Figure 3C), as they behave similarly to the non-assembling free dyes. The fluorescence emission of the donor stays obviously greater than the emission of the acceptor, lending itself to a low FRET ratio. In a disassembled/fully dynamic system the FRET ratio would not be expected to change. The FRET ratio observed remains constant, however it is not at zero due a small proportion of formed conjugates.

In water, which is less hydrogen bond competitive than DMF, the solvent molecules can still compete with peptide-peptide hydrogen bonding, however to a far lesser extent than in DMF. The increase in FRET ratio (Figure 3C) shows that the dye conjugates are dynamically exchanging to form

increasingly mixed tubular aggregates. The plateau reached after 3 hours shows that no further net mixing occurs after this point (Figure 3C).

Surprisingly, this dynamic behaviour was also observed in toluene where the solvent is not expected to compete with the hydrogen bond stacking sites of the CP. As expected, the rate at which they exchange is far slower than in water (7 days compared to 3 hours). In non-polar solvents the solvent molecules do not interact with the hydrogen bond sites on the cyclic peptide. For this reason, a slow rate of dynamics in toluene can be seen in both the kinetic rate constants (Table 2). As the solvent is able to interfere with hydrophibic interactions between CP, potentially weakening the connection, a possible mechanism for this is that the nanotubes are breaking at different positions and reform instead of the exchange of unimers.[32]

The maximum FRET ratio was determined by measuring a premixed system. This was prepared by first separately dissolving each dye conjugate in DMF and then mixing them in a 1:1 ratio. The solvent was then evaporated and the residual CP conjugates were re-dissolved in water or toluene (Figure 4A). This ensured that the nanotubes formed in solution would be random supramolecular copolymers of both compounds. The minor difference observed between the maximum and final FRET ratio could be associated to the presence of small homogenous regions within the nanotubes.

Table 2. The rate kinetics of the exchanging donor and acceptor conjugated cyclic peptide-polymer nanotubes. The final FRET ratio was the value at which the plateaux was reached.

Solvent	K_1/ s^{-1}	K_2/ s^{-1}	Final FRET ratio	Max FRET ratio*	Degree of mixing/ %
DMF	-	-	0.084	0.084	(100%)
Water	96.12	3.80	0.729	0.810	90%
Toluene	1.10	0.06	0.780	0.882	88%

* The maximum FRET ratio was determined using a premixed sample dissolve in the respective solvent. See experimental section for details.

The FRET ratio calculated for the free dyes in water was constant at 0.857 due to a small degree of direct excitation of the acceptor. Similarly in DMF, no emission change over time and a low FRET ratio indicates these conjugates resemble the free dyes and not aggregates.

A theoretical FRET ratio of 1 would be expected if the dye conjugates formed statically mixed tubes of infinite length. Shown in Table 2, the final FRET ratios observed do not reach 1, therefore, suggesting the length of the aggregates formed, or the presence of unimers in solutions, prevents a quantitative exchange.

Concentration dependency of CPNT self-assembly

The described FRET system was also used to study the effect of concentration on the assembly of the CPNTs. Using the premixed system in water, *vide supra*, the solution was systematically diluted to observe the influence of concentration on the nanotube assembly. The fluorescence acceptor emission of this solution was measured upon excitation at 500 nm (donor) and 677nm (acceptor) independently. The FRET intensity was normalised against the maximum emission determined by direct excitation of the acceptor. As expected, the normalised FRET intensity decreased upon dilution (Figure 4B). Interestingly, at low concentrations, a plateau was reached, after which further dilution of the system showed no change in normalised FRET emission.

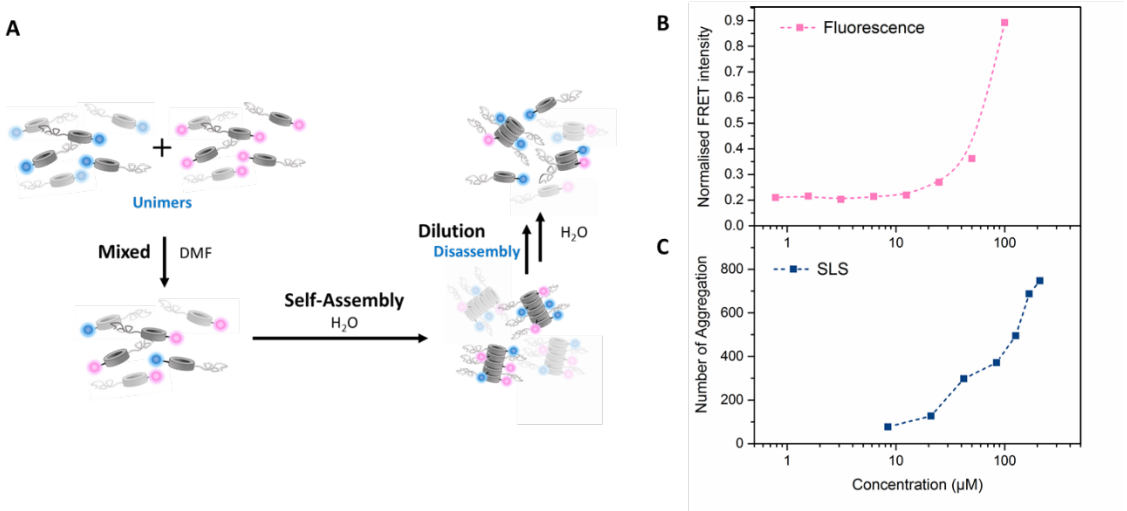

Figure 4. A) Fluorescence emission concentration dependent study of the mixed nanotubes. The concentration dependence on the cyclic peptide (premixed PEG-CP-Cy3 and PEG-CP-Cy5) stacking measured *via* B) fluorescence microscopy of the premixed dye conjugates and C) SLS of the control conjugates.

Using static light scattering (SLS) the average molecular weight and N_{agg} of non-dye conjugates were studied in a similar concentration regime as the FRET study with the dye conjugates (Figure S16). This is corroborated by SANS which showed similar nanotubular lengths for the premixed dye and non-dye conjugates. A trend, whereby at lower concentrations a decrease in the number of aggregation, was observed in the SLS. It should be noted that these scattering experiments only yield relative information about these systems, as these values may be an effect of interactions between tubes at higher concentrations. Nevertheless, the relative observations of the polymerization process as observed from SLS supports the trend as obtained by FRET, whereby at lower concentrations smaller aggregates were formed (Figure 4C). Aggregation of the conjugates at lower concentrations could not be studied accurately using SLS due to insufficient intensity of scattered

***In vitro* dynamic of cyclic peptide nanotubes**

Having characterised the dynamics of these model cyclic peptide-polymer conjugates in a controlled environment (i.e. pure water), we turned to studying their behaviour in a more complex setting, namely living biological systems. The peptides PEG-CP-Cy3 and PEG-CP-Cy5 were incubated in the presence of MDA-231 cells (human breast adenocarcinoma) and fluorescence, including FRET-associated fluorescence, was observed using fluorescent confocal microscopy. PEG-CP-Cy3 was used in a higher concentration (12 μM) than PEG-CP-Cy5 (4 μM) to account for the lower intensity as a result of not exciting the dye at its absorption maximum, resulting in a total concentration of 16 μM peptide. Negative controls whereby the cells were incubated individually with either PEG-CP-Cy3 or PEG-CP-Cy5 for 150 minutes clearly showed intracellular fluorescence when excited at their respective dye absorption and observed at their respective dye emission (Figure 5). The vast majority of the fluorescence can be observed in the intracellular region close to the nucleus, in a punctuated

design which indicates that the compounds have not diffused in the cytosol but remain trapped within the lysosomes instead. Endosomal uptake and subsequent localisation in the lysosomes is expected for such nanosized objects and has been demonstrated for similar structures.[33]

When both PEG-CP-Cy3 **10** and PEG-CP-Cy5 **11** were co-injected and co-incubated in the presence of cells, allowing cyclic peptide-polymers to form mixed conjugates before or during cell entry, fluorescence associated with FRET could be observed within the cells. A similar result was observed when PEG-CP-Cy3 and PEG-CP-Cy5 where premixed in DMF, dried, re-dissolved in water, and injected in the cell culture. These results indicate that synthesised nanotubes of mixed conjugates can enter cells *via* endocytosis and remain intact within the harsh environment of the lysosomes for the time of the study.

Next, we wanted to test whether individual CPs could form mixed conjugates within the complex environment of living cells. We hypothesized that PEG-CP-Cy3 and PEG-CP-Cy5 nanotubes incubated separately with the cells could, given enough time, mix within the restricted environment of the lysosomes. By incubating PEG-CP-Cy5 for 30 minutes, washing the cells thoroughly and further incubating with PEG-CP-Cy3 for 120 minutes, a significant increase in the intracellular fluorescence associated with FRET as compared to the control was observed (Figure 5E-F). This result clearly indicates that not only some of the nanotubes are transported into the same cell compartment but that the nanotubes are still able to exchange and re-organise themselves into mixed self-assembled systems within the cells. Given the low initial concentration of PEG-CP-Cy3/Cy3 and the small distance required for an energy transfer, this finding is very likely a result of co-stacking. Taken together, the data demonstrate that this self-assembling system is robust enough to maintain its shape within a biological environment whereas the dynamic character is preserved enabling difference species of nanotubes to communicate with each other *via* the exchange of unimers. The compatibility of these nanostructures with living cells highlights the potential of these compounds for future biological and biomedical applications.

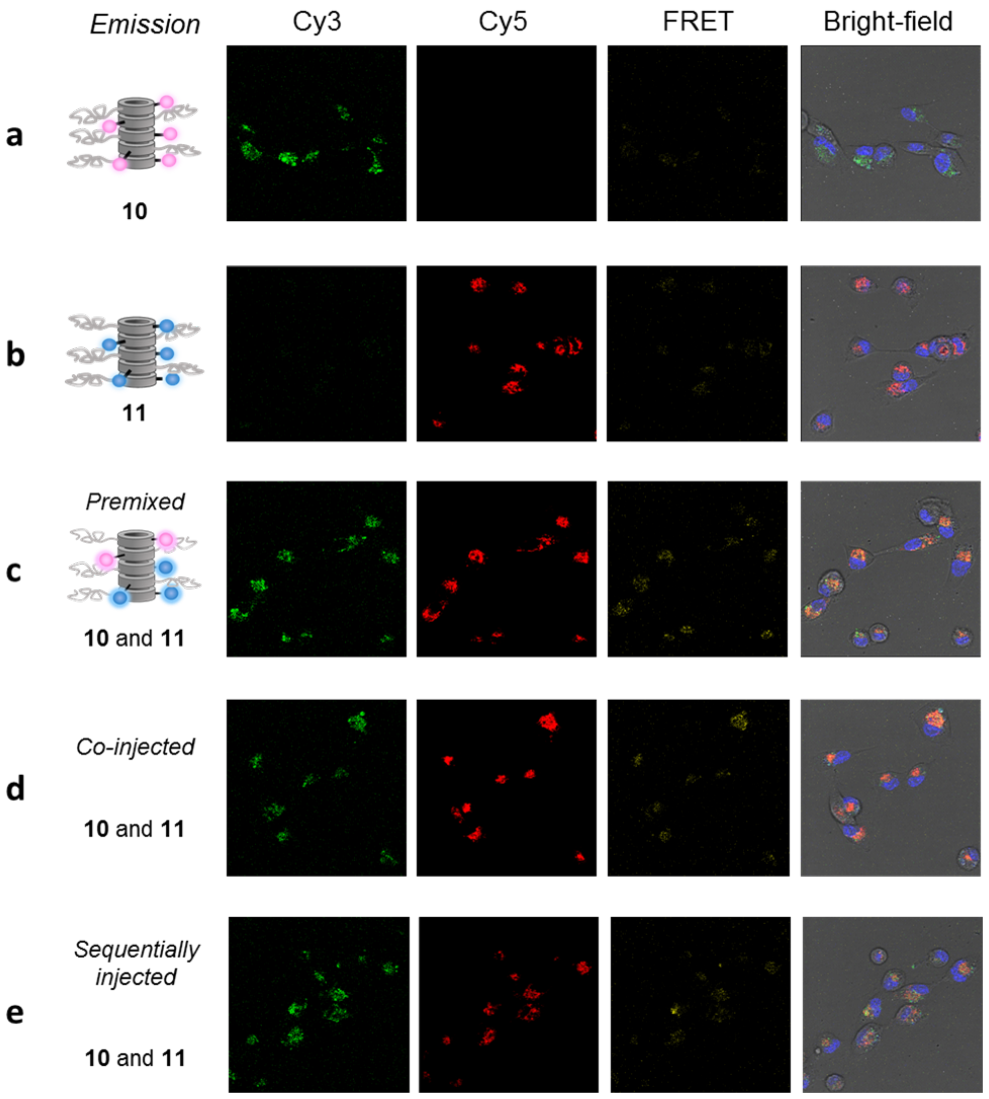
Emission
Cy3
Cy5
FRET
Bright-field
a
10
b
11
Premixed
c
10 and 11
Co-injected
d
10 and 11
Sequentially injected
e
10 and 11

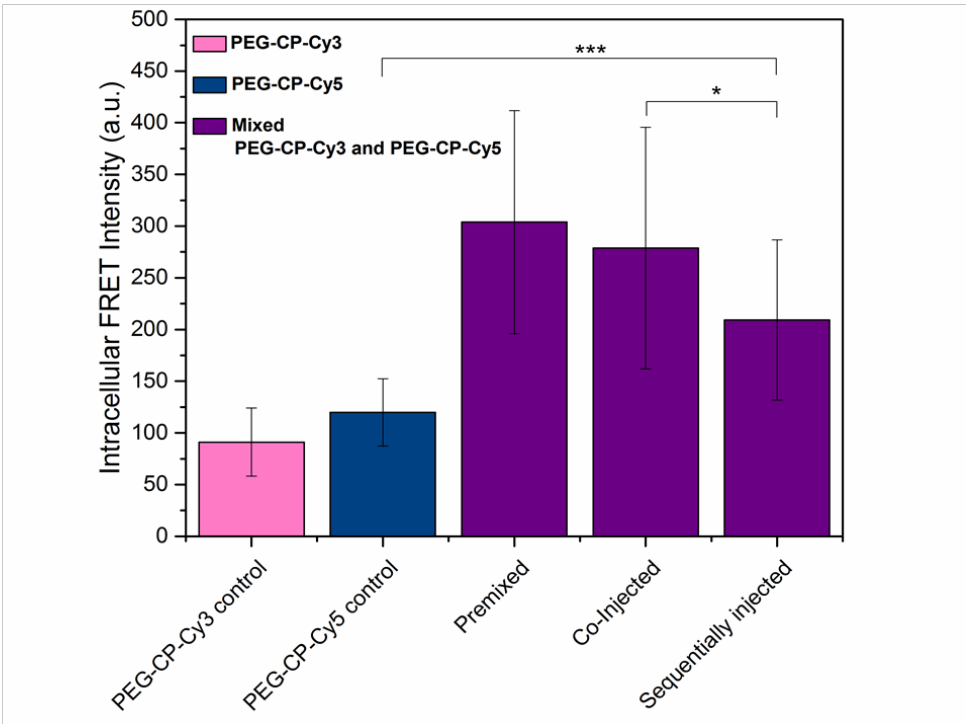
PEG-CP-Cy3
PEG-CP-Cy5
Mixed
PEG-CP-Cy3 and PEG-CP-Cy5
***
*
Intracellular FRET Intensity (a.u.)
0
50
100
150
200
250
300
350
400
450
500
PEG-CP-Cy3 control
PEG-CP-Cy5 control
Premixed
Co-Injected
Sequentially injected

Figure 5. Confocal microscopy imaging of MDA-231 cells incubated in the presence of either A) PEG-CP-Cy5 alone (4 μM); B) PEG-CP-Cy3 alone (12 μM); C) premixed PEG-CP-Cy5 (4 μM) and PEG-CP-Cy3 (12 μM); D) co-injected PEG-CP-Cy5 (4 μM) and PEG-CP-Cy3 (12 μM); E) PEG-CP-Cy5 (4 μM) for 30 minutes, washed and PEG-CP-Cy3 (12 μM) for 120 minutes. Unless indicated otherwise, incubation proceeded for 150 min. Nucleus fluorescence was obtained using Hoechst 33342. Excitation/Emission used for measurement are as follow, nucleus channel (405 / 406-459 nm), donor channel (517 / 540-577 nm), acceptor channel (633 / 670-724 nm), FRET (496 / 675-800 nm). F) Average intensity of intracellular fluorescence associated with FRET, as calculated using the mean of fluorescence in each cells for a minimum of 15 cells.

Conclusion

In this study, Förster Resonance Energy Transfer was used as a tool to demonstrate the dynamic behaviour of self-assembling cyclic peptide-polymer nanotubes in polar and non-polar environments. The same system was also used to study the aggregation at very low concentration as well as in the complex environment of living cells. Mixing the readily assembled nanotubes resulted in a time dependent increase in energy transfer associated with FRET, which proves that these supramolecular systems were readily exchanging units and are not kinetically trapped in various solvents of different polarity. Although in all cases near quantitative mixing is observed in comparison to premixed samples; the kinetics are much faster in aqueous solutions as compared to toluene. Further studies showed that upon dilution the fluorescence associated with the FRET decreased which is related to steady decrease in size of the aggregates, a trend confirmed *via* static light scattering. In complex environments such as living cells, the combination of FRET and confocal microscopy showed that the different nanotubes were independently transported into the same cell compartments addition of the individual FRET-dye conjugates. This ability to recombine even under such conditions as present in living cells makes these materials attractive as a basic system for tracking of transport pathways, especially as further ligands can easily be attached to the polymer chain. In general, the obtained results provide the first fundamental information about the dynamic nature of these promising supramolecular systems in a range of different environments and lay the basis for further investigation

on manipulating these dynamics and so far unanticipated applications of these nanotubes for example as sensor devices and biological trackers.

Associated content

Electronic supplementary information

Experimental section

Materials

Fmoc-protected amino acids and coupling agents were purchased from Iris Biotech GmbH. Cyanine3 NHS ester and Cyanine5 NHS ester were obtained from Lumiprobe GmbH, Germany. The amine functionalised PEG was purchased from Rapp Polymere. Pentanoic acid was purchased from Alfa Aesar (UK).

All other chemicals stated were purchased from Sigma-Aldrich, (Gillingham, UK) unless otherwise stated. Solvents were purchased from several departmental suppliers – Honeywell, Fisher and Sigma Aldrich.

Characterisation

Nuclear magnetic resonance spectroscopy (NMR)

^{1}H NMR spectrum were measured using a Bruker DPX-300 or DPX-400 NMR spectrometer which operated at 300.13 and 400.05 MHz respectively. The residual solvent peaks were used as internal references. Deuterated trifluoroacetic acid (*d*-TFA) (δ_H = 11.5 ppm) was used to measure the peptides.

Size-exclusion chromatography (SEC) / Gel permeation chromatography (GPC)

GPC was measured using an Agilent PL50 instrument with a differential refractive index (DRI) detector. The instrument contained two PolarGel H columns (300 x 7.5 mm) and a PolarGel 5μm guard column. DMF with 0.1% LiBr additive was used as the eluent. The system ran at 1mg min^{-1}

(50ºC), with an injection volume of 100 µL. The samples were prepared by filtering them through 0.22 µm pore size membranes, before injection. Agilent EasyVial poly (methyl methacrylate) standards were used to calibrate the instrument and output data was analysed using Agilent GPC/SEC software.

Small Angle Neutron Scattering (SANS)

SANS was carried out on the Sans2d small-angle diffractometer at the ISIS Pulsed Neutron Source (STFC Rutherford Appleton Laboratory, Didcot, U.K.).[34] A simultaneous Q-range of 0.0045 – 0.7 $Å^{-1}$ was achieved utilizing an incident wavelength range of 1.75 – 16.5 Å and employing an instrument set up of L1=L2=4m, with the 1 m^2 detector offset vertically 60 mm and sideways 100 mm. Q is defined as:

$$Q = \frac{4\pi \sin\frac{\theta}{2}}{\lambda} \qquad (2)$$

where θ is the scattered angle and λ is the incident neutron wavelength. The beam diameter was 8 mm. Each raw scattering data set was corrected for the detector efficiencies, sample transmission and background scattering and converted to scattering cross-section data ($\partial\Sigma/\partial\Omega$ vs. Q) using the instrument-specific software.[35] These data were placed on an absolute scale (cm^{-1}) using the scattering from a standard sample (a solid blend of hydrogenous and perdeuterated polystyrene) in accordance with established procedures.[36] Conditions and experimental information can be found in the supplementary information, S17.

Ultraviolet/visible (UV-Vis) absorption spectroscopy

UV-Vis absorption spectra was measured using an Agilent Technologies Cary 60 UV-Vis spectrometer. The UV spectra of PEG-CP-Cy3 (**10**) and PEG-CP-Cy5 (**11**) were obtained in each

solvent (water, DMF, toluene). The solution were all made to the same concentration (35 μM). Spectra can be found in the supplementary information, Figure S10.

Fluorescence emission spectroscopy

Fluorescence emission spectra was measured using an Agilent Technologies Cary Eclipse Fluorescence spectrometer.

The FRET studies were performed using an excitation wavelength of 500 nm. This was done to significantly reduce the direct excitation of the acceptor in the FRET studies. The acceptor emission upon excitation at 500 nm was considerably smaller than at 548nm (absorption maxima of the donor). See figures S10 and S11 in the supplementary information for the absorption and emission spectra, respectively, of the conjugates **10** and **11**.

Dynamics in self-assembled systems

First, 35 μM stock solutions of PEG-CP-Cy3 and PEG-CP-Cy5 were prepared in the water. The emission spectra of the PEG-CP-Cy3 was measured before the addition of the PEG-CP-Cy5 conjugate. The fluorescence emission spectra were taken using the Agilent Kinetic software. Excitation of the donor was set to 500 nm, donor emission (detected) to 565 nm and acceptor emission (detected) at 662 nm. The mixing of the dyes Cy3-NHS and Cy5-NHS were also tested using the same conditions.

Solvent dependence study

First, 35 μM stock solutions of PEG-CP-Cy3 and PEG-CP-Cy5 were prepared in the relevant solvent. The emission spectra of the PEG-CP-Cy3 was measured before the addition of the PEG-CP-Cy5 conjugate. The fluorescence emission spectra were taken at several time points upon the addition of the PEG-CP-Cy5. The FRET ratio was obtained using the equation 1, the relative FRET intensities were calculated and fitted to a second order exponential function.

Concentration dependence study

First, 50 μM stock solutions of PEG-CP-Cy3 and PEG-CP-Cy5 in DMF were prepared. 1 mL of each stock solution was added to a vial and the solution was shaken for 30 minutes and the solvent was evaporated. The residual solid was then redissolved in a precise volume of water (around 1 mL) to create a dye conjugate solution with a concentration of 100 μM. 1 mL of this solution was transferred to measure the first concentration (100 μM). Next, 1 mL of water was added to the cuvette to yield the next dilution (50 μM). For subsequent concentrations the solution in the cuvette was transferred to another vial and further dilution concentrations were made up in a new vial using 1 mL of water and 1 mL of the transferred (previous) solution.

High performance liquid chromatography (HPLC)

High performance liquid chromatograms (HPLC) was measured using an Agilent Technologies 1200 Series, equipped with a Luna 5u C18 100 Å, 250 x 4.6mm column. Acetonitrile/Water were used. All solvents contained 0.04 vol% TFA. Further information about the method and gradients can be found with the HPLC data in the supplementary information - Figure S3, S7~9.

Mass spectrometry (ESI-TOF)

Electronspray ionisation (ESI) – time of flight (TOF) mass spectra (MS) was measured using a Bruker MicroTOF to characterise the peptides and peptide conjugates. The instrument can achieve less than 5 ppm mass accuracy.

Static Light Scattering (SLS)

The SLS data were obtained using the ALV/CGS-3 Compact Gonimeter System.

A range of different concentrations of non-dye conjugated CP-polymers measured using SLS. The compounds were first accurately measured in a vial and corresponding volumes of water were added to yield various different concentrations (5 mg mL^{-1} - 0.2 mg mL^{-1}). Before measuring, the solutions

were filtered using 0.2 µM membrane PTFE lined filters to remove any large PEG crystalline aggregates.

Confocal microscopy

MDA-231 (human breast adenocarcinoma) cells were cultured in High Glucose DMEM medium supplemented with 10% fetal bovine serum. For confocal microscopy, MDA-231 cells were seeded in an 8-well ibidi plate at a density of 10 000 cells per well and allowed to grow for 48 hours prior to the experiment. Cells medium was then replaced by fresh medium and supplemented with PEG-CP-Cy5 (4 µM), PEG-CP-Cy5 (12 µM), or both, from stock solutions at 200 µM in water. For the premixed sample, stock solutions of PEG-CP-Cy5 (200 µM) and PEG-CP-Cy5 (600 µM) were prepared in DMF, sonicated, DMF evaporated with N_2 flow and re-dissolved in water. Cells were incubated with conjugates for 135 minutes. In the case of sequential incubation, PEG-CP-Cy5 (4 µM) was incubated first for 30 minutes, the cells washed thoroughly with PBS, then incubated with fresh media and PEG-CP-Cy5 (12 µM) for 105 minutes. For all sample, Hoechst 33342 was then added and incubation proceeded for another 15 minutes before cells were washed with warm media twice. Confocal microscopy images were taken on a Leica TCS SP5 (Carl Zeiss, Germany) at a temperature of 37°C, using sequential scanning for each channel. Excitation/Emission used for measurement are used as follow: nucleus channel (405 / 406-459 nm), donor channel (517 / 540-577 nm), acceptor channel (633 / 670-724 nm), FRET (496 / 675-800 nm). Average of fluorescence for each sample was measured using ImageJ software by isolating single cells as region of interest and averaging the mean of fluorescence in each cells, on a minimum of 15 cells by samples.

Transmission Electron Microscopy (TEM)

Carbon films (4 nm) were prepared on freshly cleaved mica sheets using a Quorum Q150T Turbo carbon coater. These films were deposited on copper TEM girds (mesh 400 – Agar Scientific) by flotation water. Solutions of PEG-CP-dye/alkyl conjugates in water at 1 mg mL^{-1} were prepared by direct dissolution of the solid in filtered ultra-pure water. Samples were left to age for 24h at room temperature then filtered through PTFE syringe filters (0.45 µm pore size). 10 µL of each solution was

drop-cast on freshly glow-discharged carbon-coated grids placed on filter paper. After drying, 10 μL of a 2% uranyl acetate solution in ethanol was dropped onto the grids on filter paper and left to dry. Bright field TEM micrographs were obtained with a JEOL 1400 microscope operating at 120 kV, equipped with a Gatan digital camera.

Synthesis

The synthesis of the cyclic peptide N_3-CP-NH_2 (**3**)and the azido-modified Fmoc-protected amino acid was synthesised. Standard deprotection solid phase peptide synthesis was used to first synthesis the protected linear peptide. Using a coupling agent the cyclisation was completed in dilute conditions to avoid intermolecular reactions. The insolubility of the stacked cyclic peptides in methanol was used to isolate the pure cyclic peptide. The cyclic peptide was then deprotected using TFA to reveal the amine of the lysine and azoles on the tryptophans. Characterisation of the linear peptide and cyclic peptide can be found in the supplementary information, S1.

Conjugation of the dye to the cyclic peptide

CP-Cy3 (4): The cyclic peptide **4** (20.0 mg, 1.66 x 10^{-5} mol, 1 eq.) was dissolved in DMF (0.5 mL) with the aid of sonication. To make certain the amine on the cyclic peptide was deprotected N,N-Diisopropylethylamine (DIPEA) (10 $mgmL^{-1}$ stock solution in DMF, 0.64ml of stock solution, 6.4 mg, 4.98 x 10^{-5} mol, 3 eq.) was added. The solution was shaken for 30 minutes. The Cyanine3 NHS ester (11.6 mg, 1.99 x 10^{-5} mol, 1.2 eq.) was then added to the solution and shaken overnight. The product was purified *via* precipitation using THF. Yield: 67% (18.5mg, 1.12 x 10^{-5} mol). ESI-ToF, m/z (found) = 1644.9, (calculated) = 1645.0 ($[M]^+$), see figure S4. HPLC (t_R= 24 mins) using Acetonitrile/Water gradient. Spectra and gradient information can be found in the supplementary information, S7.

CP-Cy5 (5): CP-Cy5 (**5**) was synthesised using the same protocol as CP-Cy3 (**4**). Cyanine5 NHS ester was used instead of Cyanine3 NHS ester to synthesise **5**. Yield: 29% (8.2 mg, 4.9 x 10^{-6} mol). ESI-ToF, m/z (found) = 1671.2, (calculated) = 1671.0 ($[M]^+$), see figure S5. HPLC (t_R= 24 mins) using Acetonitrile/Water gradient. Spectra and gradient information can be found in the supplementary information, S8.

Conjugation of pentanoic acid to the cyclic peptide

CP-Alkyl (6): Pentanoic acid (2.7 µL, 2.49 x 10^{-5} mol, 3 eq.), HCTU (10.3mg, 2.49 x 10^{-5} mol, 3 eq.) and N,N-Diisopropylethylamine (DIPEA) (6.43 mg, 4.97 x 10^{-5} mol, 6 eq.) were dissolved together in DMF (1 mL) and shaken for 10 minutes. The cyclic peptide **4** (10.0 mg, 8.29 x 10^{-6} mol, 1 eq.) was separately dissolved in DMF (0.5 mL) with the aid of sonication. The pentanoic acid mixture was then added to the cyclic peptide solution. The resultant solution was shaken for 3 hours. The product was purified *via* precipitation using ice-cold diethyl ether. Yield: 61% (4.68 mg, 1.12 x 10^{-5} mol). ESI-ToF, m/z (found) = 1312.5, (calculated) = 1312.8 ($[M+Na]^+$), see figure S6. Due to the insolubility of this compound HPLC was not possible.

NHS functionalisation of the cyclic peptide conjugates (CP-Cy3, CP-Cy5 and CP-alkyl)

NHS-CP-Cy3 (7): The CP-Cy3 (**4**) (18.5 mg) was dissolved in DMF (0.5 mL) with the aid of sonication. (1R,8S,9s)-Bicyclo[6.1.0]non-4-yn-9-ylmethyl N-succinimidyl carbonate (BCN-NHS) was added to the cyclic peptide solution. The resultant solution was shaken overnight. The product was purified *via* precipitation using ice-cold diethyl ether. Yield: 73% (17.8 mg, 9.19 x 10^{-6} mol). ESI-ToF, m/z (found) =1936.0, (calculated) = 1936.1 ($[M]^+$), see figure S4. HPLC (t_R= 22 mins) using Acetonitrile/Water gradient. Spectra and gradient information can be found in the supplementary information, S7.

NHS-CP-Cy5 (8): NHS-CP-Cy5 (**8**) was synthesised using CP-Cy5 (**5**) and the same protocol as NHS-CP-Cy3 (**7**). Yield: 78% (7.9 mg, 4.0 x 10^{-6} mol). ESI-ToF, m/z (found) =1962.1, (calculated) =

1962.1 ($[M]^+$), see figure S5. HPLC (t_R= 22 mins) using Acetonitrile/Water gradient. Spectra and gradient information can be found in the supplementary information, S8.

NHS-CP-Alkyl (9): NHS-CP-Alkyl (**6**) was synthesised using CP-Alkyl (**6**) and the same protocol as NHS-CP-Cy3 (**7**). Yield: 74% (4.1 mg, 2.6 x 10^{-6} mol). Due to the insolubility of this compound ESI-ToF and HPLC was not possible.

Conjugation of the polymer to the cyclic peptide

PEG-CP-Cy3 (10): NHS-CP-Cy3 (**7**) (14mg) was dissolved in DMF (0.5mL) with the aid of sonication. α-Methoxy-ω-amino PEG 20 kDa (0.247 g, 1.08 x 10^{-5} mol, 1.5 eq.) was added to the cyclic peptide solution. To make certain the amine on the polymer was deprotected N,N-Diisopropylethylamine (DIPEA) (10mg/mL stock solution in DMF, 0.24 ml of stock solution, 2.4 mg, 1.4 x 10^{-5} mol, 2 eq.) was added. The solution was shaken overnight. The product was purified using centrifuge dialysis tubes with a molecular weight cut-off of 50kDa. Yield: 58% (101 mg, 4.21 x 10^{-6} mol). HPLC (t_R= 16 mins) using Acetonitrile/Water gradient. Spectra and gradient information can be found in the supplementary information, S7.

PEG-CP-Cy5 (11): PEG-CP-Cy5 (**11**) was synthesised using NHS-CP-Cy5 (**8**) and the same protocol as PEG-CP-Cy3 (**10**). Yield: 67% (59.9 mg, 2.48 x 10^{-6} mol). HPLC (t_R= 16 mins) using Acetonitrile/Water gradient. Spectra and gradient information can be found in the supplementary information, S8.

PEG-CP-Alkyl (12): PEG-CP-Cy5 (**12**) was synthesised using NHS-CP-Alkyl (**9**) and the same protocol as PEG-CP-Cy3 (**10**). Yield: 56% (34.4 mg, 1.45 x 10^{-6} mol). HPLC (t_R= 21 mins) using Acetonitrile/Water gradient. Spectra and gradient information can be found in the supplementary information, S9.

Acknowledgements

We thank the Royal Society Wolfson Merit Award (WM130055; SP), the Monash-Warwick Alliance (SP; JR) and the European Research Council (TUSUPO 647106; SP) for funding. MH (DFG, GZ: HA

7725/1-1) and JB (DFG, GZ: BR 4905/1-1 and BR 4905/2-1) gratefully acknowledge the German Research Foundation for funding. ISIS, UK is thanked for allowing us X-press time on the Sans2D instrument. LRM would like to acknowledge the Electron Microscopy Unit at the University of Bristol for use of TEM instruments.

References

[1] a) S. Arber, F. A. Barbayannis, H. Hanser, C. Schneider, C. A. Stanyon, O. Bernard, P. Caroni, *Nature* **1998**, 393, 805; b) H. Fraenkel-Conrat, R. C. Williams, *Proc. Natl. Acad. Sci. U. S. A.* **1955**, 41, 690.

[2] a) D. Li, Y. Xia, *Adv. Mater.* **2004**, 16, 1151; b) J. D. Hartgerink, E. Beniash, S. I. Stupp, *Science* **2001**, 294, 1684.

[3] M. R. Ghadiri, J. R. Granja, R. A. Milligan, D. E. McRee, N. Khazanovich, *Nature* **1993**, 366, 324.

[4] X. Wang, G. Guerin, H. Wang, Y. Wang, I. Manners, M. A. Winnik, *Science* **2007**, 317, 644.

[5] S. Yagai, Y. Monma, N. Kawauchi, T. Karatsu, A. Kitamura, *Org. Lett.* **2007**, 9, 1137.

[6] a) S. R. Diegelmann, J. M. Gorham, J. D. Tovar, *J. Am. Chem. Soc.* **2008**, 130, 13840; b) A. P. H. J. Schenning, E. W. Meijer, *Chem. Commun.* **2005**, 26, 3245-3258.

[7] M.-C. Daniel, D. Astruc, *Chem. Rev.* **2004**, 104, 293.

[8] Y. Bae, S. Fukushima, A. Harada, K. Kataoka, *Angew. Chem.* **2003**, 115, 4788.

[9] T. Aida, E. W. Meijer, S. I. Stupp, *Science* **2012**, 335, 813.

[10] M. M. J. Smulders, M. M. L. Nieuwenhuizen, T. F. A. de Greef, P. van der Schoot, A. P. H. J. Schenning, E. W. Meijer, *Chem. - Eur. J.* **2010**, 16, 362.

[11] T. F. A. De Greef, M. M. J. Smulders, M. Wolffs, A. P. H. J. Schenning, R. P. Sijbesma, E. W. Meijer, *Chem. Rev.* **2009**, 109, 5687.

[12] L. Pauling, R. B. Corey, H. R. Branson, *Proc. Natl. Acad. Sci. U. S. A.* **1951**, 37, 205.

[13] D. A. Fletcher, R. D. Mullins, *Nature* **2010**, 463, 485.

[14] a) E. D. Spoerke, S. G. Anthony, S. I. Stupp, *Adv. Mater.* **2009**, 21, 425; b) R. Chapman, M. Danial, M. L. Koh, K. A. Jolliffe, S. Perrier, *Chem. Soc. Rev.* **2012**, 41, 6023; c) A. M. Sanders, T. J. Magnanelli, A. E. Bragg, J. D. Tovar, *J. Am. Chem. Soc.* **2016**, 138, 3362.

[15] V. Dartois, J. Sanchez-Quesada, E. Cabezas, E. Chi, C. Dubbelde, C. Dunn, J. Granja, C. Gritzen, D. Weinberger, M. R. Ghadiri, *Antimicrob. Agents Chemother.* **2005**, 49, 3302.

[16] a) K. Motesharei, M. R. Ghadiri, *J. Am. Chem. Soc.* **1997**, 119, 11306; b) M. Danial, C. M.-N. Tran, K. A. Jolliffe, S. b. Perrier, *J. Am. Chem. Soc.* **2014**, 136, 8018.

[17] B. M. Blunden, R. Chapman, M. Danial, H. Lu, K. A. Jolliffe, S. Perrier, M. H. Stenzel, *Chem. - Eur. J.* **2014**, 20, 12745.

[18] P. Somerharju, *Chem. Phys. Lipids* **2002**, 116, 57.

[19] F. Wurthner, *Chem. Commun.* **2004**, 14, 1564-1579.

[20] R. J. Brea, M. E. Vázquez, M. Mosquera, L. Castedo, J. R. Granja, *J. Am. Chem. Soc.* **2007**, 129, 1653.

[21] R. Roy, S. Hohng, T. Ha, *Nat. Meth.* **2008**, 5, 507.

[22] a) M. G. J. ten Cate, N. Severin, H. G. Börner, *Macromolecules* **2006**, 39, 7831; b) J. Couet, J. D. J. S. Samuel, A. Kopyshev, S. Santer, M. Biesalski, *Angew. Chem. Int. Ed.* **2005**, 44, 3297.

[23] J. C. Brendel, G. Gody, S. Perrier, *Polym. Chem.* **2016**, 7, 5536.

[24] M. J. Hollamby, *PCCP* **2013**, 15, 10566.

[25] a) M. L. Koh, P. A. FitzGerald, G. G. Warr, K. A. Jolliffe, S. Perrier, *Chem. - Eur. J.* **2016**, 22, 18419; b) R. Chapman, G. G. Warr, S. Perrier, K. A. Jolliffe, *Chem. - Eur. J.* **2013**, 19, 1955; c) S. Catrouillet, J. C. Brendel, S. Larnaudie, T. Barlow, K. A. Jolliffe, S. Perrier, *ACS Macro Lett.* **2016**, 5, 1119.

[26] M. Engels, D. Bashford, M. R. Ghadiri, *J. Am. Chem. Soc.* **1995**, 117, 9151.

[27] E. A. Jares-Erijman, T. M. Jovin, *Nat. Biotech.* **2003**, 21, 1387.

[28] T. Förster, *Ann. Phys.* **1948**, 437, 55.

[29] a) M. R. Ghadiri, J. R. Granja, L. K. Buehler, *Nature* **1994**, 369, 301; b) J. D. Hartgerink, J. R. Granja, R. A. Milligan, M. R. Ghadiri, *Journal of the American Chemical Society* **1996**, 118, 43.

[30] R. Chapman, M. L. Koh, G. G. Warr, K. A. Jolliffe, S. Perrier, *Chemical Science* **2013**, 4, 2581.

[31] a) S. I. S. Hendrikse, S. P. W. Wijnands, R. P. M. Lafleur, M. J. Pouderoijen, H. M. Janssen, P. Y. W. Dankers, E. W. Meijer, *Chem. Commun.* **2017**, 53, 2279; b) C. Pietsch, U. S. Schubert, R. Hoogenboom, *Chem. Commun.* **2011**, 47, 8750.

[32] L. Albertazzi, D. van der Zwaag, C. M. Leenders, R. Fitzner, R. W. van der Hofstad, E. Meijer, *Science* **2014**, 344, 491.

[33] M. Chemerovski-Glikman, E. Rozentur-Shkop, M. Richman, A. Grupi, A. Getler, H. Y. Cohen, H. Shaked, C. Wallin, S. K. T. S. Wärmländer, E. Haas, A. Gräslund, J. H. Chill, S. Rahimipour, *Chem. - Eur. J.* **2016**, 22, 14236.

[34] a) R. Heenan, S. Rogers, D. Turner, A. Terry, J. Treadgold, S. King, *Neutron News* **2011**, 22, 19; b) ISIS Science & Technology Facilities Council, http://www.isis.stfc.ac.uk, accessed.

[35] Mantid Project, http://www.mantidproject.org, accessed.

[36] G. T. Wignall, F. Bates, *J. Appl. Crystallogr.* **1987**, 20, 28.